HYDROGEN, FUEL CELL & ENERGY STORAGE

Innovative Shell-and-Tube Heat Exchanger Design for Automotive Radiator Replacement: A Novel Approach to Replacing Car Radiators

Amin Eskandari | Faramarz Ranjbar* | Moharram Jafari | Faramarz Talati

Department of Mechanical Engineering, University of Tabriz, Tabriz, Iran
* Corresponding author, Email: s.ranjbar@tabrizu.ac.ir

Article Information

Article Type
Research Article

Article History
Received: *09 Aug 2025*
Revised: *10 Oct 2025*
Accepted: *11 Oct 2025*
Published Online: *08 Nov 2025*

Keywords

Compact heat exchanger
Shell-tube heat exchanger
Dynamic analysis
Radiator

Abstract

A radiator is a crucial component of the engine's cooling system, responsible for dissipating heat from a mixture of antifreeze and water. It releases excess heat while allowing cool air to pass through before circulating the cooled fluid back to the engine. One of the challenges of using a radiator is its installation location in different vehicles. In passenger cars and trucks, the radiator is typically positioned at the front of the vehicle. As a result, in front-end collisions, this compact and delicate heat exchanger is highly susceptible to severe damage. Additionally, the leakage of coolant from the damaged radiator can further compromise the vehicle's functionality. The purpose of this research is to introduce a new system consisting of a shell-tube heat exchanger that replaces the traditional radiator while performing the same cooling function. This system is designed with consideration of existing radiator-related issues, aiming to improve both volume efficiency and safety. In this study, a low-error simulation was conducted for the Om457-946 diesel engine produced by IDEM Tabriz Company, which has a test report and an accurate performance curve. The results indicate that the heat load at no load and 900 rpm is 65.3125, while at full engine load and 2000 rpm, it reaches 120.9513. Additionally, the designed shell-and-tube heat exchanger model has a 46% smaller volume compared to the current radiator.The shell-and-tube heat exchanger is generally cylindrical in shape, but in this study, the proposed exchanger is designed as a rectangular cube, taking into account computational coefficients, pressure drop, and shape considerations. This design change is one of the innovative aspects of the research. However, the methods and equations used remain consistent with conventional shell-and-tube exchangers. Another novelty of the research is that it increases the radiator's resistance while simultaneously reducing its volume.

Cite this article: Eskandari, A., Ranjbar, F., Jafari, M., Talati, F. (2025). Innovative Shell-and-Tube Heat Exchanger Design for Automotive Radiator Replacement: A Novel Approach to Replacing Car Radiators. DOI: 10.22104/hfe.2025.7378.1341

 Publisher: Iranian Research Organization for Science and Technology (IROST)
DOI: 10.22104/hfe.2025.7378.1341

1 Introduction

A radiator is a heat exchanger used to transfer thermal energy from one medium to another for cooling and heating. The majority of radiators are constructed to use in cars, buildings, and electronics. They act as a source of heat to their surroundings, either to heat an environment or to cool the fluid or coolant circulating through them, as seen in automotive engine cooling systems and HVAC dry cooling towers. Despite their name, most radiators primarily transfer heat through convection rather than thermal radiation.

Radiators are used for cooling internal combustion engines, mainly in automobiles but also in piston-engined aircraft, railway locomotives, motorcycles, stationary generating plants, and other applications where heat engines are used. In contrast, watercraft typically use liquid-liquid heat exchangers instead of radiators, as they have an unlimited supply of relatively cool water outside. Although the radiator, due to its location in most land vehicles, is the most susceptible component to damage in road accidents, changing its design and installation location to incorporate a heat exchanger may be a viable solution. This approach could help prevent radiator damage during accidents and may prove to be the only feasible option for enhancing vehicle durability in such situations. A heat exchanger is a system used to transfer heat between a source and a working fluid. Heat exchangers are used in both cooling and heating processes [1]. The fluids may be separated by a solid wall to prevent mixing, or they may be in direct contact [2]. They are widely used in space heating, refrigeration, air conditioning, power stations, chemical plants, petrochemical plants, petroleum refineries, natural gas processing, and sewage treatment. The classic example of a heat exchanger is found in an internal combustion engine in which a circulating fluid known as engine coolant flows through radiator coils and air flows past the coils. This process cools the coolant and heats the incoming air. Another example is a heat sink, which is a passive heat exchanger that transfers heat generated by an electronic or mechanical device to a fluid medium, often air or a liquid coolant [3].

The use of a shell-tube heat exchanger has no limitations in terms of installation location. The main difference lies in the use of a radial fan instead of an axial fan. This shaft can either be directly connected to the engine water pump shaft or powered by a separate electric motor. Given the performance standards of engine centrifugal pumps, which typically provide a head pressure of around 6 psi, the pressure drop of the proposed heat exchanger is fully accommodated. Radial fans are capable of generating a maximum head of 300 millimeters of water. Under no-load conditions, when the vehicle is stationary, the primary limitation is the airflow pressure drop within the heat exchanger, which will be optimized in future calculations for this section. However, when the vehicle is in motion and the engine RPM increases, the increase in head is first evaluated using the similarity principle for incompressible flow turbomachines. Additionally, the dynamic head of the air entering the engine compartment can also be utilized to enhance performance.

The assumption of incompressible airflow, even at high speeds and low temperatures, is based on the fact that the Mach number of the airflow is less than 0.3. For heavy-duty trucks operating at high torque and low speeds, the pressure drop in the heat exchanger, filter, and air passages can still be effectively managed. As a result, the current radiator dimensions can be maintained, even with the presence of the air conditioning condenser. The airflow caused by the truck's movement can be channeled, and the dimensions can be adjusted on the opposite side to create an air duct. While maintaining the allowed flow velocity, this modification will provide sufficient dynamic head before entering the fan. The fan head is then added, covering all pressure drops. Future calculations will be presented in tables and diagrams, followed by discussion and conclusions.

2 Literature Review

Heat exchangers are almost the most widely used component in physical and chemical processes. They can be seen in most industrial units. They facilitate heat transfer between liquid-liquid, gas-gas, or gas-liquid systems. Heat exchangers are utilized across a wide range of applications. These applications include power plants, refineries, petrochemical industries, building and production facilities, process industries, food and pharmaceutical industries, metal smelting, as well as heating, ventilation, air conditioning, refrigeration systems, and space applications. Various devices such as boilers, steam generators, condensers, evaporators, coolers, cooling towers, fan coil pre-heaters, oil coolers, heaters, radiators, furnaces, etc. all function as types of heat exchangers [1]. Heat exchangers are among the most critical equipment in power plants and refineries, playing a key role in heating or cooling process fluids. In fact, a distillation column in a refinery consists of multiple heat exchangers. Their significance lies in ensuring that process fluids reach the required temperature conditions; failure to do so can disrupt the operation of refineries and industrial or chemical units [2]. The wide range of applications for high-pressure heat exchangers necessitates a detailed study and analysis of their specific characteristics, especially when com-

pared to other types, from an engineering perspective. Therefore, this section will present several studies and works conducted in the field of heat exchangers. Shell and tube heat exchangers, for example, can be classified based on various criteria: (1) Type and contact surface of hot and cold fluids, (2) Flow direction of hot and cold fluids, (3) Heat transfer mechanism between fluids, and (4) Mechanical structure and construction of exchangers [3].

Shell and tube heat exchangers are the most common and widely used non-fired heat transfer equipment in various industries. Their unique design allows them to withstand high pressures and temperatures exceeding 30 bar and 260 °C. The tubes, which can be finned or unfinned, are arranged parallel to the longitudinal axis of the shell. A shell and tube heat exchanger consists of a cylindrical shell housing tubes inside. The tubes are connected at both ends to perforated plates known as tube sheets. As the tubes pass through the system, they are held in place by a series of plates called baffles, which direct the shell-side fluid to flow perpendicular to the tubes. The combination of tubes and baffles forms what is called the tube bundle. Tie rods and spacers are used to secure the tube bundle in place. Fluids enter and exit the tubes via special channels referred to as fixed heads and floating heads, which are sometimes also referred to as inlet and outlet heads [4]. The choice of heat exchanger type depends on factors like ease of cleaning, temperature difference predictability, and the effects of expansion and contraction on the tube bundle, shell, and other internal connections. Boot et al. investigated a coil heat exchanger under sudden changes in water flow rate and derived formulas for the time constant [5]. Pearson examined a double-pipe heat exchanger, focusing on step changes in the inlet temperature of one fluid stream [6].

Heidi examined the same situation with step changes in the inlet temperature of both water and air streams. He derived the governing equations and analyzed their impact on temperature and flow rate [7]. Ratzle and Schwan used different flow distribution models on the shell side to analyze the transient behavior of a heat exchanger due to step changes in the inlet temperature of both fluids. They considered both co-current and counter-current flow configurations [4]. The governing equations were solved using the Laplace transform. The study investigated the effects of uneven flow distribution near the shell walls and the influence of the shell wall's heat capacity on the system's transient behavior. Results indicated that the Nusselt number (Pe) quantifies the impact of uneven flow distribution, which remains constant over time but becomes negligible after a certain threshold time (z). This threshold is determined by parameters such as the Nusselt number (Pe), the Number of Transfer Units (NTU), and other factors [8]. Ataer et al. studied the dynamic behavior of finned-tube heat exchangers. They investigated the effect of a step change in water inlet temperature on the exchanger's response using three methods. In the first method, they ignored the heat capacity of the fins and tube walls.

In the second method, they assumed the heat capacity of the fins and tube walls to be identical, while in the third method, they considered them separately. Assuming a constant temperature difference between the inlet and outlet of both fluids, the researchers applied energy conservation equations and solved them numerically to analyze the system's response to step changes in water inlet temperature. They then compared the results from each method with experimental data. The results obtained from Method 3, which considered separate heat capacities, matched the experimental data most closely [9].

In a separate study, they examined time delay and the time required to reach a steady state, proposing a method to analyze the transient performance of the heat exchanger in response to changes in inlet air temperature, air velocity, and water flow rate. Additionally, they analyzed the transient behavior of finned-tube heat exchangers using an approximate method [10]. Sharifi et al. investigated the transient behavior of a plate-and-frame heat exchanger subjected to step changes in water inlet temperature. They used a lumped parameter model to simulate the temperature profiles along the flow channels. The model's results were then compared with experimental data for both steady-state and transient conditions. The lumped parameter model they developed is a generalized approach applicable to analyzing the transient behavior of various plate-and-frame heat exchangers, regardless of their size [11]. Grittoff et al. conducted a comparative study of steady-state and transient methods for measuring local heat transfer [12]. They found that the results obtained under steady-state conditions were more consistent with numerical predictions [12]. Lou and Ratzlaff explored the transient behavior of finned-plate heat exchangers under sudden changes in fluid temperatures. They formulated the governing equations for the problem and solved them using the Laplace transform method after non-dimensionalizing the equations. For aluminum finned-plate heat exchangers, the transverse thermal resistance in the fins was assumed to be negligible. The authors also stated that the solution method could be extended to other types of heat exchangers, with the governing equations being easier to solve for non-finned heat exchangers [13].

Ranong and Ratzlaff investigated the steady-state and transient behavior of two coupled heat exchang-

ers with different inlet and outlet flow arrangements. They employed the Laplace transform method to analyze and solve the effect of flow rate and inlet temperature variations on the heat exchanger performance. Their findings revealed that in plate-fin heat exchangers, the fins and separator plates exhibit distinct transient thermal behaviors, leading to lateral heat conduction in the fins [14]. Ribeiro et al. presented a numerical solution for the steady-state simulation of plate heat exchangers (PHEs). Their method considered various flow configurations including countercurrent, concurrent, or a combination of these patterns arranged in series or parallel. They validated their numerical results by comparing them with analytical solutions for simple cases and experimental data. The authors successfully applied their algorithm to simulate an industrial PHE used for milk pasteurization, demonstrating the effectiveness of their approach [15].

In this study, considering that in a car crash, the radiator – positioned at the front of the vehicle – is quickly damaged, leading to coolant leakage and eventual engine failure, a new cooling system design is proposed. Based on previous research, this article presents a coolant cooling heat exchanger that can be installed in an alternative location within the vehicle. This design not only reinforces the water tank but also ensures the proper functioning of the cooling system, preventing engine failure and vehicle stoppage.

3 Explanation of the Problem

3.1 Assumptions

1. Steady-state analysis
2. The heat exchanger calculations are performed for the engine idle state, which represents the lowest airflow rate. These calculations serve as a baseline for evaluating the heat exchanger's performance under different engine speeds and loads.
3. According to the relevant standard, the coolant exiting the engine thermostat is set at 180 °F, while the return coolant temperature from the radiator is 170 °F. The coolant flow rate is determined based on engine test data and the corresponding heat load of the coolant.
4. The ambient conditions for the airflow (considered the cool fluid) are assumed to be standard. This corresponds to an absolute pressure of 1 atmosphere (325 kPa or 24.6 psi) and a temperature of 25 °C (77 °F).
5. The heat exchanger design was optimized while considering limitations on airflow pressure drop, overall heat exchanger dimensions (assumed to be a rectangular box shape), water flow velocity (between 4 and 8 fps), and head velocity (between 25 and 40 m/s). After performing calculations, the most suitable configuration was found to be water flowing through the tubes and air flowing inside the shell of the heat exchanger.

3.2 Experimental results

According to Table 1, which summarizes the Euro IV engine test results for OM456 type 649 and 945 engines produced by IDeM Tabriz under license from Daimler-Chrysler Germany, the following engine heat loads will be used for further calculations: No-load condition: 3125 kW at 900 RPM Full-load condition: 9513 kW at 2000 RPM

Table 1. Summary of test results for motor heat load

Cooling water Heat (kW)	Thermal efficiency (%)	Heat Production (kW)	Fuel consumption mass flow rate (kg/s)	Specific fuel consumption (gr/kW.hr)	Power (kW)	Torque (N.m)	RPM	Motor type
OM457(956)	900	1260	118.7	200	0.006	276.5	42.95	65.31
	1300	1250	170.1	194	0.009	384.1	44.29	93.59
	1700	1210	215.4	198	0.011	496.3	43.10	118.5
	2000	1050	219.9	223	0.013	570.7	38.53	120.9
OM457(945)	900	1550	146.08	200	0.008	340	42.96	80.34
	1300	1595	217.1	196	0.011	495.2	43.84	119.4
	1700	1430	254.5	198	0.014	586.5	43.40	140.0
	2000	1245	260.7	222	0.016	673.6	38.71	143.4

A full engine test report for the discussed engine is also provided in the appendix. This report serves as a sample and includes 5 out of 30 rows of data. Each row contains 16 columns with various engine performance parameters. The data was obtained using AVL's testing procedure in a test cell at the engine manufacturer's

facility and is labeled as a "performance test." The information in Table 1 was extracted from the data in this test report. The appendix includes an additional document besides the sample engine test report, whichprovides performance characteristics for two OM457 engine types. This document includes graphs that show brake power, brake torque, and specific fuel consumption as functions of engine speed.

Table 2 shows the results of tests measuring the radiator outlet water temperature and the water temperature returning to the engine. The table includes data from five performance test runs at four different engine speeds. Additionally, the average temperatures for each engine speed are calculated and displayed in the table.

Table 2. Test results of cooling water returning to motor (radiator outlet)

RPM	1st test	2nd test	3rd test	4th test	5th test	Average
900	79.00	76.00	73.50	74.40	74.10	75.40
1300	77.50	76.35	76.00	74.45	74.35	75.73
1700	76.70	77.96	75.90	76.72	74.7	76.40
2000	78.00	78.20	77.80	77.50	75.00	76.50
Total Average						76.033

Based on the data in Table 2, the average engine return coolant temperature is 76.77 degrees Celsius. This temperature is somewhat influenced by the temperature of the test cell. However, when compared to the reference temperature of 170 °F, the error is less than 1%.

4 Governing Equations

Based on the average standard inlet and outlet temperatures of the engine coolant, and using the properties of water from relevant tables, the water flow rate can be calculated in the following manner using the principle of energy conservation in a steady state.

$$Q_{\mathrm{cc}} = m_0 C_{\mathrm{pw}} \Delta T_w \tag{1}$$

Table 3 compares the measured volumetric flow rate of water in the test cell with the results calculated using Equation (2). The table shows a very small relative error between the two values, indicating good agreement between the experimental and computational methods.

Since the critical heat transfer condition for the heat exchanger occurs at engine idle speed (900 rpm), it is essential to consider the minimum allowable velocities for both the hot fluid (water) and the cold fluid (air).

$$\dot{V}_w = V_w A_c = V_w N_t \frac{\Pi}{4} D_{\mathrm{it}}^2 \,, \tag{2}$$

$$h_i = 5.678\,(0.913 - 0.42 \log D_i^2) \times (165 + 1.7 t_m) V_{\mathrm{fps}}^{0.805} \,. \tag{3}$$

Now, referring to Table 4, which contains the specifications of the heat exchanger tubes extracted from relevant standard tables, we will use the previously mentioned equations to calculate the following: the number of tubes in each water flow passage, the modified velocity of the water within the tubes (accounting for non-uniform flow distribution), and the convection coefficients, which represent the rate of heat transfer between the water and the tube surface.

The following calculations show that the air-side convection coefficient is lower than the water-side convection coefficient. This means that the air side acts as the controlling film for heat transfer. As a result, tube size has minimal impact on the overall heat transfer coefficient of the heat exchanger. Instead, the emphasis should be on maximizing the heat transfer area. The analysis of the last column in Table 4, which presents the heat transfer area per unit length per pass with a constant tube spacing factor, reveals an interesting relationship. Given a fixed heat transfer area required for airflow, the heat exchanger's width remains unchanged regardless of the tube diameter. Therefore, tube diameter selection can be based on the allowable pressure drop for airflow. In simpler terms, as long as the total heat transfer area is achieved, a wider heat exchanger with smaller tubes will perform the same as a narrower one with larger tubes. However, smaller tubes will cause a higher pressure drop for the airflow. Additionally, the airflow rate is determined based on the specified inlet and outlet temperatures.

$$\dot{Q} = m_a \dot{C}_{pa} \Delta T_a \,, \tag{4}$$

$$C_n = \dot{m}_w C_{pw} \,, \tag{5}$$

$$C_c = \dot{m}_a C_{pa} \,, \tag{6}$$

$$C = \frac{C_{\min}}{C_{\max}} \,, \tag{7}$$

$$\epsilon = \epsilon_c = \frac{t_2 - t_1}{T_1 - t_1} \,. \tag{8}$$

The ratio between the cold fluid's heat capacity flow rate and the temperature flow rate, often referred to as

the thermal efficiency in this context, is given by:

$$\mathrm{Ntu} = -\frac{1}{c}\ln\left[1 + C\ln(1-\epsilon)\right], \tag{9}$$

$$u_A = \mathrm{Ntu} C_{\min}. \tag{10}$$

The subsequent calculations indicate that, under optimal conditions – considering heat exchanger volume and sufficient heat transfer surface – a 4/3-inch pipe with short integral fins (19 fins per inch)and an inner diameter of 14 millimeters is the preferred choice. Its standard specifications before and after finning are given in Tables 5 and 6.

Table 3. Test results for cooling water mass flow rate and heating load

Motor type	RPM	Heat Load (kW)	Calculated mass flow rate of cooling water (kg/s)	Calculated volumetric flow rate of cooling (kg/s) water	measured mass flow rate of cooling water (kg/s)	Relative error (%)
OM457(945)	900	65.31	2.799	2.8817	2.88	0.0342
	1300	93.59	4.011	4.1295	4.130	0.0345
	1700	118.47	5.075	5.2273	5.229	0.0340
	2000	120.95	5.187	5.3365	5.338	0.0348

Table 4. Number of tubes in one pass and convection heat transfer coefficient dependent on tube diameter

The outer diameter of the tube (in)	BWG	Thickness of tubes	Inner diameter of pipes (in)	Number of tubes	Modified velocity (fps)	Heat transfer coefficients ($\mathrm{W/m^2\,k}$)	A_{ht}/L ($\mathrm{m^2/m}$)
3/4	18	0.049	0.65	11	3.99	7930.5	0.658
5/8	19	0.042	0.54	16	3.98	8193.4	0.797
1/2	20	0.035	0.43	25	4.03	8617.8	0.997
3/8	20	0.035	0.30	50	4.01	9078.4	1.496
1/4	20	0.028	0.19	124	3.99	9715.5	2.473

Table 5. Tube specification without fin

O.D		BWG	L		I.D		OD/ID
Inch	mm		Inch	mm	Inch	mm	
1.15	16.5	0.65	1.24	0.04	18	19.0	3/4

Table 6. Finned tube specification

Manufacturer classification	T (mm)	H (mm)	D_i (mm)	FRI	A_{of}/A_i
MLF1919135	1.35	1.175	14	19	3.5

Where ϵ is the initial thickness of the pipe, I.D. is the inner diameter of the pipe before finning, t is the thickness of the pipe from the base of the fin to the inner wall, h is the fin height, and D_i is the inner diameter of the pipe after finning. Based on the information obtained from the manufacturer of short integral finned copper tubes of Mehr Asl Tabriz Company, the necessary calculations have been performed and the geometric specifications required for fin efficiency are as follows: Finthickness in 0.5 mm and fin height is 1.175 meters according to the following equations:

$$\eta_f = tgh(ml)/(ml) = 99.88\%, \tag{11}$$

$$m = \sqrt{\frac{h_0}{k_f \zeta_f}}, \tag{12}$$

$$\eta_0 = 1 - \beta(1-\eta_f). \tag{13}$$

The calculation of the convection coefficient (h_{conv}) for hot water flowing inside the pipes requires consideration of the minimum allowable velocity of 4 feet per second.

$$\dot{w}_w = N_t \frac{\pi}{4} D_{\mathrm{it}}^2 V, \tag{14}$$

$$\mathrm{Ntu} = 15, \tag{15}$$

$$h_i = 8352. \tag{16}$$

Using the Jakob experimental correlation for staggered tube banks:

$$\Delta p = \frac{2 f G_{\max}^2 N_{\mathrm{row}}}{pt}\left(\frac{M_w}{M_b}\right)^{0.14}, \tag{17}$$

$$f = \left[0.25 + \frac{0.118}{\left(\frac{s_n}{d} - 1\right)^{1.08}}\right] \mathrm{Re}_{f,\max}^{-0.16}, \tag{18}$$

$$\frac{M_w}{M_b} = \frac{0.0452 t_w + 17.307}{0.0452 t_b + 17.307}, \tag{19}$$

$$t_b = t_m = 32.5^{\mathrm{oc}}, \tag{20}$$

$$P_b = \frac{2P_i - \Delta p}{2RaTm} = \frac{P_i - \frac{\Delta P}{2}}{RaTm}, \tag{21}$$

$$P_i = P_{\mathrm{atm}} + P_{\mathrm{fan}} - \Delta P_k \tag{22}$$

$$\Delta P_k = \Delta P_{\mathrm{duck}} + \Delta P_{\mathrm{inlet}}. \tag{23}$$

ΔP_{duck} the pressure drop in the air duct from the fan outlet to the inlet header of the heat exchanger, along with the dynamic head corresponding to the discharge velocity of the heated air into the atmosphere should also be taken into account. However, in general, neglecting these factors will not significantly impact the specific gravity. Ignoring the resistance of the pipe wall and fouling resistances, the wall temperature can be estimated as follows as an initial reliable estimate:

$$t_w = \frac{h_i A_i t_{bi} + h_o t_{bo}}{h_i A_i + h_o A_o}. \tag{24}$$

Since the outer surface is finned, it is essential to account for the ratio of the outer to inner surface areas as well as the overall efficiency of the outer surface in the heat transfer calculations.

$$t_w = \frac{h_o \left(\frac{A_o}{A_i}\right) \eta_o t_{bo} + h_i t_{bi}}{h_o \left(\frac{A_o}{A_i}\right) \eta_o + h_i}, \tag{25}$$

$$t_f = \frac{1}{2}(t_w + t_{bo}), \tag{26}$$

$$\mathrm{Nus}_o = \frac{h_o D_o}{k_f} = c(\mathrm{Re}_{f,\max})^n \mathrm{Pr}_l^{\frac{1}{3}}. \tag{27}$$

From now on proper constraints will be applied:

1. The maximum air velocity between the pipes should not exceed 25 meters per second. Therefore, when determining the width and length of the opposing surface, the volumetric airflow rate must be considered to ensure compliance with this limit.
2. The minimum allowable water velocity of 4 meters per second will be the determining factor for calculating the number of pipes in each water flow passage.
3. Maximum pressure drop of the water flow concerning the heat transfer duty of the heat exchanger and taking into account the pressure drop in the transfer and circulation paths between the passages must not exceed 6 psi.

The maximum pressure drop of the airflow, considering the appropriate longitudinal and transverse pitch for the pipes, as well as the maximum heat exchange duty, must not exceed 300 mm-WG. This includes accounting for the pressure drop along the airflow path, changes in direction, and the transition of the air carrier diameter to the exchanger inlet section. Given the aforementioned constraints and solving the system of equations derived from the heat transfer, heat exchanger surface area, heat exchange duty, and flow pressure drop, interpolation using Grimmison & Jakob's multipliers for a staggered tube array configuration is required. This leads to the results given in Table 7 for the minimum cooling capacity of the heat exchanger.

Table 7.

S_n/d	S_p/d	C	N	N_{row}
2.5	1.25	0.5775	0.559	10
W	L	N_t	N_{pass}	N_{TPP}
38.1	65.7	75	5	15
H	D_{it}	N_{ot}	A_o/A_i	η
23.8	14	3/4	3.5	0.999
R	R_{di}	H_o	H_i	V_{ma}
0.001	0.0005	231.45	8352	24.99

Also, it can be said that:

$$u_o = \left[\frac{1}{n_o} + \frac{\eta_o A_0}{A_i}\frac{1}{h_i} + \frac{D_o}{2Kw}\ln\left(\frac{\eta_o A_0}{A_i}\right) + R_{do} + \left(\frac{\eta_o A_0}{A_i}\right) R_{di}\right]^{-1}, \tag{28}$$

$$u_o A_o = u_i A_i. \tag{29}$$

Using a longer length to achieve the maximum allowable flow velocity between pipes for minimum pressure drop, as per the law of conservation of mass, will result in a value of 7/65. However, this approach will also lead to an increase in sedimentation time. The novelty of this study can also be summarized as follows:

1. Freeing up the radiator installation space to create a low-temperature installation space for the car air conditioner condenser.
2. Removing the electric motor that drives the fan for airflow through the radiator, in order to create more accessible space for repairs, reduce the car's front length, and lower electrical consumption. This also enhances reliability by reducing the number of dynamic engine parts.
3. Directly connecting the radial fan to the water pump ensures that the cold and hot flows in the exchanger operate in parallel. As engine speed increases, the water pump speed rises, which boosts the cooling water flow rate. Additionally, the increased pump shaft speed causes the fan speed to increase, thereby enhancing the airflow rate.

When engine speed decreases, the opposite occurs, and the flow rates adjust in parallel. This synchronization leads to a near stabilization of the exchanger's effectiveness.

4. Replacing the radiator with a shell-and-tube heat exchanger that can be installed in various spaces around the engine ensures the engine's safety in the event of an accident. In such situations, the radiator often collapses, causing the engine's cooling water to leak and rendering the engine unable to operate, which can prevent the vehicle from moving.

5 Validation

Given that little to no similar work has been done on this subject, a dimensionless parameter, the Reynolds number, was used to validate the heat exchanger design. The results were then compared with the findings of R. Gugulothu and N. Sanke's research [16]. The results showed acceptable overlap and the calculated error percentage was 0.53%.

6 Results

Given the dimensions of the radiator window in trucks with power above 100 kW, as well as the radiator's thickness, the volume of its core is approximately 118,800 cubic centimeters. However, the proposed heat exchanger has a core volume of 5/59,575 cubic centimeters.

This implies that the total volume of the radiator, including the high and low-temperature headers, is approximately 147,690 cubic centimeters. In contrast, the proposed heat exchanger, including the water flow headers and airflow conversion channels, has a calculated volume of 124,053.6 cubic centimeters, representing a 27.19% reduction in total volume.

According to the calculations performed and the technical specifications provided by Idem Tabriz Company, a comparison of the designed dimensions of the heat exchanger with the radiator is presented in Table 8.

Table 8. Comparing the designed heat exchanger with radiator

	Length (cm)	Height (cm)	Width (cm)	Volume (cm^3)
Radiator	12	120	75	108000
Rectangular Cube cube H.E.	64	24	38	58368

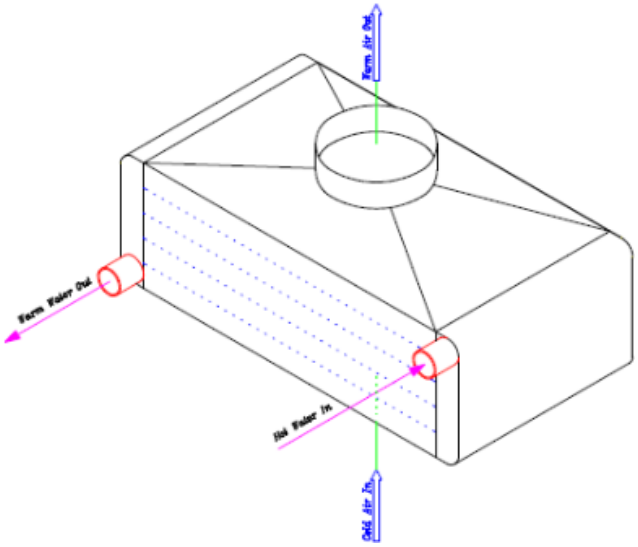

Fig. 1. Schematic of Heat Exchanger

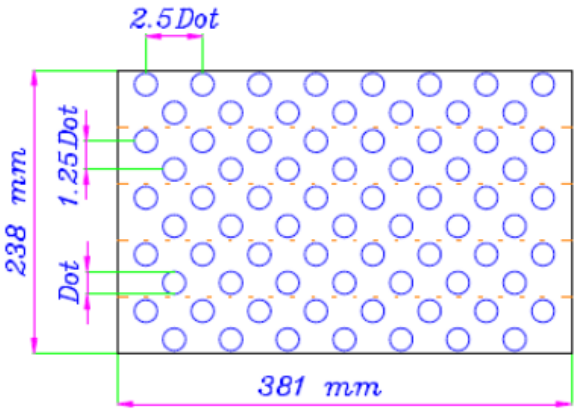

Fig. 2. Geometric specification of the heat exchanger plate

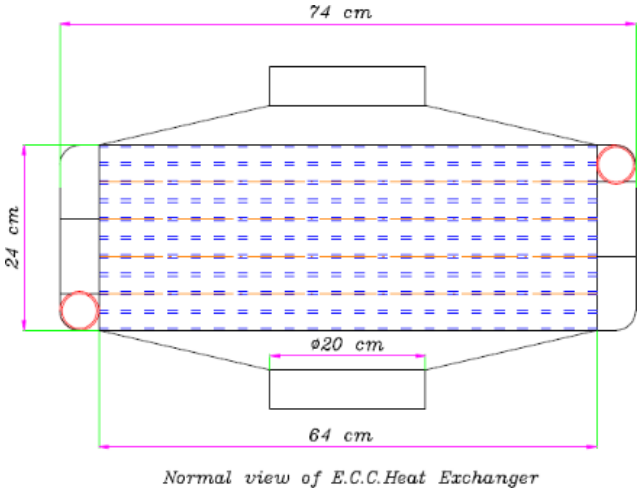

Fig. 3. Figure 3: Overal schematic of heat exchanger

This comparison clearly shows that the dimensions of the heat exchanger designed in this study are 46% smaller than those of conventional car radiators.

Calculations were performed for the maximum allowable airflow velocity of 40 meters per second and the maximum allowable water flow velocity of 8 fps. The results for both no-load and full-load engine conditions were compared, as shown in Table 9.

Table 9. The results of No load and a full load of the engine

RPM	Radiator Heat Load (kW)	Air Mass Flow Rate (kg/s)	Maximum Velocity of air (m/s)	Air Inlet temperature	Outlet Air Temperature	Pressure Drop in Air Flow Rate	Total Pressure Drop (mm wG)
900	65.31	4.33	25	25	40	85	287.3
2000	120.9	6.93	40	25	42.35	202	720.0
Efficiency of fan	Colling Water mass Flow Rate (kg/s)	The velocity of water in tubes (m/s)	Cooling water inlet temperature	Cooling water outlet temperature	Water Pressure Drop in the heat exchanger (Pa)	Total pressure drop of water (Psi)	
100	2.79	4.09	180	170	0.55	1.2	
35.5	5.18	7.59	180	170	1.90	4.3	
Water Pump Efficiency	Internal surface of heat transfer	The external surface of heat transfer	Effectiveness of external surface	Convection heat transfer coefficient of airside	Convection heat transfer coefficient of waterside	Overall heat transfer coefficient of HX	Temperature efficiency of heat exchanger
100	2.11	7.38	99.9	231.4	8352	190.3	26.21
57.8	2.11	7.38	99.9	300.9	1314.	244.3	30.23

Given that the fan generates a pressure head of 300 mm-wG, when the engine is operating at full load, the increase in speed and heat load of the replacement heat exchanger results in an additional pressure drop of approximately 420.004 mm-wG imposed on the system. This additional pressure drop must be compensated for by the dynamic head of the vehicle's speed. Calculations show that if the vehicle's speed is 60 km/h, approximately 17.7% of the radiator mounting window height should be allocated to the air inlet duct. This duct should be converted into a circular shape with a diameter of 20 cm leading to the fan inlet, thereby providing the required pressure head.

Of course, if the vehicle is moving at a higher speed, the increase in speed and pressure drop will be offset by the dynamic head generated from the airflow velocity at the fan inlet. As a result, the additional pressure drop will be compensated for, and the outlet temperature of the airflow from the heat exchanger will remain below 35.42 degrees Celsius.

7 Conclusion

The designed exchanger has a core volume of 59,575.5 cubic centimeters, while the core volume of the radiator in trucks with a power output of more than 100 kW is about 118,800 cubic centimeters, taking into account the dimensions of the radiator window and the thickness of the radiator.

This means the total volume of the cooler, including the upper and lower temperature headers, is approximately $147,690,0\,\mathrm{m}^3$, while the desired exchanger volume, including the water flow headers and air flow conversion ducts, is approximately $124,053.6\,\mathrm{m}^3$.

Given that the fan produces a pressure head of 300 mm WG, when the engine operates at full load, an additional pressure drop of approximately 420 mm WG is introduced to the system due to the increased speed and heat load of the radiator-replacing exchanger. This additional pressure drop must be compensated by the dynamic head generated by the vehicle's speed. For instance, at a speed of 60 km/h, 17.7% of the window height would need to be allocated for the airflow. Ultimately, the novelty of the present study lies in modifying the shape and volume of the radiator, optimizing its design, and enhancing its physical resistance during accidents.

References

[1] Hornyik K. Heat exchangers-thermal-hydraulic fundamentals and design. Nuclear Technology. 1982;58(3):556-6.

[2] Costa AL, Queiroz EM. Design optimization of shell-and-tube heat exchangers. Applied thermal engineering. 2008;28(14-15):1798-805.

[3] Shah R, Sekulic D. Heat exchangers. Handbook of heat transfer. 1998;3.

[4] Shah RK, Sekulic DP. Fundamentals of heat exchanger design. John Wiley & Sons; 2003.

[5] Boot J, Pearson J, Leonard R. An improved dynamic response model for finned serpentine cross flow heat exchangers. ASHRAE Trans. 1977:218-39.

[6] Pearson J, Leonard R, Mccutchan R. Gain and time constant for finned serpentine crossflow heat exchangers. ASHRAE Trans. 1974:255-67.

[7] Haidi M, Padet J. Study of a heat exchanger with variable inlet temperatures. In: Heat Transfer in Single Phase Flows Eurotherm Seminar No. 25. Universite de Pau et des pays del'Adour; 1991. p. 6. Preprint.

[8] Roetzel W, Xuan Y. Analysis of transient behaviour of multipass shell and tube heat exchangers with the dispersion model. International journal of heat and mass transfer. 1992;35(11):2953-62.

[9] Ataer ÖE, Ileri A, Göğüş Y. Transient behaviour of finned-tube cross-flow heat exchangers. International journal of refrigeration. 1995;18(3):153-60.

[10] Ataer ÖE. An approximate method for transient behavior of finned-tube cross-flow heat exchangers. International journal of refrigeration. 2004;27(5):529-39.

[11] Sharifi F, Narandji MG, Mehravaran K. Dynamic simulation of plate heat exchangers. International Communications in Heat and Mass Transfer. 1995;22(2):213-25.

[12] Critoph R, Holland M, Fisher M. Comparison of steady state and transient methods for measurement of local heat transfer in plate fin-tube heat exchangers using liquid crystal thermography with radiant heating. International journal of heat and mass transfer. 1999;42(1):1-12.

[13] Luo X, Roetzel W. The single-blow transient testing technique for plate–fin heat exchangers. International journal of heat and mass transfer. 2001;44(19):3745-53.

[14] Ranong CN, Roetzel W. Steady-state and transient behaviour of two heat exchangers coupled by a circulating flowstream. International journal of thermal sciences. 2002;41(11):1029-43.

[15] Ribeiro Jr C, Andrade MC. An algorithm for steady-state simulation of plate heat exchangers. Journal of food engineering. 2002;53(1):59-66.

[16] Gugulothu R, Sanke N. Experimental investigation of heat transfer characteristics for a shell and tube heat exchanger. Energy Harvesting and Systems. 2024;11(1):20220147.